Accepted Manuscript

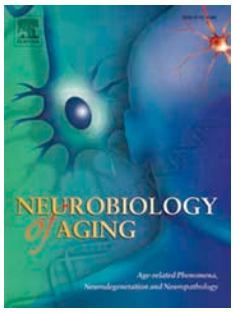

White matter integrity is associated with CSF markers of AD in normal adults

Brian T. Gold, Zude Zhu, Christopher A. Brown, Anders H. Andersen, Mary Jo LaDu, Leon Tai, Greg A. Jicha, Richard J. Kryscio, Steven Estus, Peter T. Nelson, Steve W. Scheff, Erin Abner, Fred A. Schmitt, Linda J. Van Eldik, Charles D. Smith

PII: S0197-4580(14)00337-6

DOI: 10.1016/j.neurobiolaging.2014.04.030

Reference: NBA 8864

To appear in: *Neurobiology of Aging*

Received Date: 31 October 2013

Revised Date: 23 April 2014

Accepted Date: 27 April 2014

Please cite this article as: Gold, B.T., Zhu, Z., Brown, C.A., Andersen, A.H., LaDu, M.J., Tai, L., Jicha, G.A., Kryscio, R.J., Estus, S., Nelson, P.T., Scheff, S.W., Abner, E., Schmitt, F.A., Van Eldik, L.J., Smith, C.D., White matter integrity is associated with CSF markers of AD in normal adults, *Neurobiology of Aging* (2014), doi: 10.1016/j.neurobiolaging.2014.04.030.

White matter integrity is associated with CSF markers of AD in normal adults

Brian T. Gold[a,f,h], Zude Zhu[a], Christopher A. Brown[a], Anders H. Andersen[a,f], Mary Jo LaDu[i], Leon Tai[i], Greg A. Jicha[b,h], Richard J. Kryscio[c,h], Steven Estus[d,h] Peter T. Nelson[e,h], Steve W. Scheff[a,h], Erin Abner[g,h] Fred A. Schmitt[b,h], Linda J. Van Eldik[a,h] & Charles D. Smith[b,f,h]

a Department of Anatomy and Neurobiology
b Department of Neurology
c Department of Statistics
d Department of Physiology
e Department of Pathology
f Magnetic Resonance Imaging and Spectroscopy Center
g Department of Epidemiology
h Sanders-Brown Center on Aging
University of Kentucky, Lexington, KY 40536 USA
i Department of Anatomy and Cell Biology,
University of Illinois, Chicago, IL 60612, USA

Correspondence:
Brian T. Gold
Department of Anatomy and Neurobiology,
University of Kentucky College of Medicine,
Lexington, KY, 40536-0298
Phone: (859) 323-4813
Fax: (859) 257-6700
Email:brian.gold@uky.edu

Abstract

We explored whether white matter (WM) integrity in cognitively normal (CN) older adults is associated with cerebrospinal fluid (CSF) markers of Alzheimer's disease (AD) pathology. Twenty CN older adults underwent lumbar puncture and magnetic resonance imaging within a few days of each other. Analysis of diffusion tensor imaging data involved *a priori* region of interest (ROI) and voxelwise approaches. The ROI results revealed a positive correlation between CSF measures of amyloid-beta ($A\beta_{42}$ and $A\beta_{42}$/p-Tau_{181}) and WM integrity in the fornix, a relationship which persisted after controlling for hippocampal volume and fornix volume. Lower WM integrity in the same portion of the fornix was also associated with reduced performance on the Digit Symbol test. Subsequent exploratory voxelwise analyses indicated a positive correlation between CSF $A\beta_{42}$/p-Tau_{181} and WM integrity in bilateral portions of the fornix, superior longitudinal fasciculus, inferior fronto-occipital fasciculus, and in the corpus callosum and left inferior longitudinal fasciculus. Our results link lower WM microstructural integrity in CN older adults with CSF biomarkers of AD and suggest that this association in the fornix may be independent of volumetric measures.

Keywords: Normal older adults, CSF, white matter, DTI, preclinical AD

1. Introduction

Alzheimer's disease (AD) is the most common cause of dementia, affecting more than 5 million Americans and placing enormous strain on the US health care system. It is known that AD neuropathology is present years before cognitive symptoms associated with clinical AD (Bennett, et al., 2006, Morris, et al., 1996). Motivated by this knowledge and an impending rise in cases of AD, clinical diagnostic criteria have recently been revised to emphasize the need for biomarkers that can detect preclinical stages of AD (McKhann, et al., 2011, Sperling, et al., 2011). These revised diagnostic criteria focus primarily on AD-related protein biomarkers such as amyloid-beta and tau in cerebral spinal fluid (CSF) and brain imaging indices of gray matter (GM) structure and metabolism.

There has been relatively less focus on the potential for white matter (WM) integrity biomarkers in preclinical AD. However, increasing evidence suggests pathological alterations to WM microstructural integrity in AD. For example, partial loss of myelin sheaths, axons, and oligodendroglial cells has been reported in patients with AD (Brun and Englund, 1986, Englund, 1998, Ihara, et al., 2010). Convergent evidence of WM integrity disruption in AD has been demonstrated by diffusion tensor imaging (DTI), an *in vivo* method for characterizing the microstructural properties of WM by measuring the rate and direction of diffusion of water molecules trapped in neural tissue (Basser, et al., 2000, Beaulieu, 2002, Le Bihan, 2003, Moseley, 2002). A body of data from DTI studies has demonstrated that reduced WM integrity is evident in AD and its typical prodromal state of amnestic mild cognitive impairment (aMCI) (reviewed in Stebbins and Murphy, 2009).

More recently, WM integrity reductions have been observed in multiple DTI studies of cognitively normal (CN) individuals at high AD-risk based on genetics and/or family

history (reviewed in Gold, et al., 2012). However, it remains unclear if lower WM integrity in CN older adults is associated with CSF measures of AD pathology such as $A\beta_{42}$ or p-Tau_{181}. Accumulating evidence suggests a potential link between WM integrity and these CSF measures of AD pathology. For example, Aβ deposits have been shown to be cytotoxic to oligodendrocytes in vitro (Xu, et al., 2001) and increased levels of Aβ peptides have been associated with reduced levels of myelin biochemical markers at autopsy in patients with AD (Roher, et al., 2002). The aggregation of abnormally hyperphosphorylated tau may also affect WM microstructure given that tau binds to and stabilizes microtubules, which are essential for structural integrity and axonal transport (Shahani and Brandt, 2002).

Here we sought to determine if lower WM integrity in CN individuals is associated with CSF markers of AD pathology. CSF biomarkers of AD are thought to precede neuroimaging alterations by several years (Jack, et al., 2010). Thus, to maximize power to detect subtle CSF-DTI correlations in CN individuals, our primary analyses employed an ROI approach (although additional voxelwise analyses were also performed) focusing on two limbic tracts known to be affected in early stages of AD: the fornix and cingulum. Reduced WM integrity in the fornix has been found in individuals with familial autosomal dominantly inherited forms of AD (Ringman, et al., 2007) and in individuals at high genetic risk for sporadic AD (Gold, et al., 2010). Reduced WM integrity in the cingulum has been observed in multiple studies of individuals at high genetic and/or familial risk for sporadic AD (Bendlin, et al., 2010, Heise, et al., 2011, Persson, et al., 2006, Smith, et al., 2010).

The fornix and cingulum have direct connections with GM structures known to undergo neurodegenerative changes early in the course of AD. The fornix is the principal efferent tract of the hippocampus, and the cingulum is one of the main tracts associated

with the entorhinal cortex (ERC). The volume of the hippocampus and ERC are reduced in individuals with aMCI and AD (Convit, et al., 1997, Jack, et al., 1997) and in CN individuals destined for future aMCI or AD (Apostolova, et al., 2010, Dickerson and Wolk, 2012, Martin, et al., 2010). Thus, we controlled for the volume of these GM structures in our WM integrity—CSF analyses. In addition, fornix WM integrity analyses controlled for fornix volume to determine if DTI measures reveal unique information not captured by macrostructural measures of this tract.

2. Methods

2.1. Participants

Twenty CN older adults (8 male, 12 female) participated in this study. Participants were recruited from an existing cohort of cognitive normal volunteers who undergo annual collection of demographic, health, and neuropsychologic data and blood samples as part of an ongoing longitudinal study of aging (Schmitt, et al., 2012). Exclusionary criteria applied at intake for the longitudinal study are history of substance abuse, traumatic brain injury, major psychiatric illness, medical illnesses that are unstable (requiring other than routine follow-up and medical management) and/or have an effect on the central nervous system (e.g., encephalitis, meningitis, stroke, multiple sclerosis, epilepsy, Parkinsonism, or other neurologic disease). Continued diagnosis of cognitive normality by the UK-ADC clinical core was based on a uniform set of clinical assessment procedures common to United States ADCs described in detail elsewhere (Morris et al., 2006). This includes collection of the Uniform Data Set (UDS), collected from all ADC subjects and shared with the National Alzheimer's Coordinating Center (NACC) in Seattle, Washington, under an agreement with

the National Institute on Aging (NIA) Alzheimer's Centers Program. Neuropsychological test results from the current UDS battery (Weintraub, et al., 2009) available for all subjects in the present study were the Mini Mental State Examination (MMSE), verbal fluency (VF animals), Trail Making Tests (Trails) A and B, Immediate (LM Imm) and Delayed (LM Del) recall of Logical Memory Paragraph of the Wechsler Memory Scale-Revised, and Wechsler Adult Intelligence Scale-Revised Digit Symbol (DS).

Participants in the present study were those who agreed to lumbar puncture as part of a pilot study that seeks to explore the relationship between CSF and imaging markers of AD. Exclusion criteria for the present MRI-CSF study beyond those applied for entry into our longitudinal cohort were claustrophobia, pacemakers, or the presence of metal fragments and/or metallic implants contraindicated for MRI. Characteristics of the participants are shown in Table 1. Written informed consent was obtained from each participant under an approved University of Kentucky Institutional Review Board protocol.

2.2. Cerebrospinal fluid collection and analysis

Lumbar CSF was drawn the morning after fasting since midnight using a 20-gauge needle, 15-mL sterile polypropylene collection tubes, and was maintained in single-use 0.5 ml aliquots in polypropylene storage tubes in a -80°C freezer. CSF samples were shipped on dry ice from the University of Kentucky to the LaDu laboratory at the University of Illinois at Chicago for analysis. $A\beta_{1\text{-}42}$ and phosphorylated-tau_{181} (p-tau_{181}) were measured using INNOTEST® ELISA kits (Innogenetics, Gent, Belgium) according to the manufacturer's protocol with 21F12 antibody for capture and 3D6 (biotinylated) antibody for detection of $A\beta_{1\text{-}42}$, and antibodies HT7 for capture and AT270 for detection of P-tau_{181}. All samples

were split into two volumes for each assay to allow for duplicate runs. Prior to analysis, samples were kept frozen at all times and were thawed just before testing.

2.3. MRI acquisition procedures

The majority of participants were scanned on the same day as their lumbar puncture (Mean gap = 2 days; SD =6.4) and within 3 months of their cognitive testing (Mean gap = 84.9 days; SD =71.8). Imaging data were collected on a Siemens Trio TIM 3 Tesla scanner at the Magnetic Resonance Imaging and Spectroscopy Center of University of Kentucky using a 32-channel head coil. High-resolution, three-dimensional anatomic images were acquired using a magnetization prepared rapid acquisition with gradient echo (MP-RAGE) sequence [repetition time (TR) = 2530 ms, echo time (TE) = 2.26 ms, inversion time (TI) = 1100 ms, flip angle = 7°, acquisition matrix = 256×256×176, field of view (FOV) = 256 mm, isotropic 1 mm voxels]. Diffusion tensor imaging (DTI) used a double spin echo planar imaging (EPI) sequence acquired with 64 non-collinear encoding directions (b = 1000 s/mm^2) and seven images without diffusion weighting (b = 0 s/mm^2, b_0). The cerebrum was covered using 52 contiguous 2-mm thick axial slices (TR = 8000 ms, TE = 96 ms, FA = 90°, acquisition matrix = 112×112, FOV = 224 mm, yielding isotropic 2 mm voxels).

2.4. *DTI analysis*

Diffusion tensor imaging (DTI) data were processed and analyzed using FSL's FMRIB software library (FSL v4.1.5). Raw images were pre-processed to correct for motion and residual eddy current distortion using a 12-parameter affine alignment to the corresponding $b0$ image via FMRIB's Linear Image Registration Tool (FLIRT: http://www.fmrib.ox.ac.uk/fsl). Brain masks were then generated from each $b0$ image

using FMRIB's brain extraction tool (BET v2.1) to exclude non-brain voxels from further consideration (Smith, et al., 2006). Next, FMRIB's Diffusion Toolbox (FDT v2.0) was used to fit the diffusion tensor and calculate eigenvalues, fractional anisotropy (FA), mean diffusivity (MD), axial diffusivity (DA) and radial diffusivity (DR).

Registration of FA images into MNI152 space and subsequent voxelwise analyses followed a series of procedures known as Tract-Based Spatial Statistics [TBSS v1.2; (Smith et al., 2006) http://www.fmrib.ox.ac.uk/fsl/tbss/], as described in detail in our previous work (Johnson, et al., 2012). Briefly, the first step in this process was to remove likely outliers from the fitted tensor data by eroding brain edge artifacts and zeroing the end slices. Second, all subjects' FA images were aligned to a target (the one to which the least amount of warping is required) using a nonlinear registration approach based on free-form deformations and B-Splines (Rueckert et al., 1999). FA datasets were then affine registered and resampled to 1 × 1 × 1 mm MNI152 space. The exact transformations derived from the FA maps were then applied to the other diffusivity maps (MD/DR/DA) for matched processing of all image volumes. All subsequent processing was carried out in MNI space.

All MNI-transformed FA images were then averaged to generate a mean FA image that was used to create a common WM tract skeleton. This skeleton was then thresholded at an FA value of 0.2 to minimize partial voluming effects after warping across subjects. Each participant's aligned FA image was subsequently projected onto the FA skeleton to account for residual misalignments between participants after the initial nonlinear registration. Each subject's MD, DA and DR maps in MNI space were then projected onto the common tract skeleton, using the pipeline for non-FA data provided by TBSS, which

employs the projection vectors from each individual's FA-to-skeleton transformation (Smith et al., 2006).

A priori ROI analyses. The motivation for an initial *a priori* ROI analysis was twofold. First, we expected subtle effects in CN older adults and thus attempted to maximize power by centering our ROIs around WM regions previously linked with high AD-risk. Second, we sought to replicate effects in specific ROIs in MNI space on a different group of CN older adults, toward a long-term goal of the development of potential biomarkers of AD. Two *a priori* ROIs were selected for correlations with CSF analytes. The WM ROIs were portions of the left fornix and left cingulum (Figure 1), and were centered around peak MNI coordinates of WM integrity reductions in CN individuals at high AD-risk in our previous study (Gold, et al., 2010). The ROIs were situated within a ventro-caudal portion of the fornix (in the crus region; MNI coordinates: -27 -25 -4) and a ventro-caudal portion of the cingulum (MNI coordinates: -22 -27 -18). The ROI masks were 3 mm isotropic cubes surrounding these peak coordinates. Each ROI was masked with the mean FA skeleton in order to minimize partial voluming. The means from these clusters (e.g., mean FA) were extracted from each participant using FSL's utility 'fslmeants'.

_____

Figure 1 about here

_____

2.5. *Hippocampal and ERC volumes*

The hippocampus and ERC were selected for correlations with CSF analytes. In contrast to our WM ROIs, we had no specific peak MNI coordinates to guide selection of GM volumetric ROIs. Thus, our GM ROIs were derived anatomically. FreeSurfer software

(http://surfer.nmr.mgh.harvard.edu) was used for cortical parcellation (Desikan, et al., 2006, Fischl, et al., 2004) and subcortical segmentation (Fischl, et al., 2002). The standard data processing stream in FreeSurfer was used for removal of the B1 bias field, skull stripping, segmentation and GM volume labeling. Anatomical structure volumes were 'normalized' (divided by intracranial volume; ICV), providing an estimate of atrophy in that ROI.

2.6. *Fornix volume*

Left fornix volume was computed to determine if correlations between CSF measures of Aβ and WM microstructural integrity in our left fornix ROI persisted after controlling for volume in this structure. The procedure involved warping of the left fornix mask from the International Consortium of Brain Mapping (ICBM) DTI WM labels atlas onto each participants T1 image in order to compute volumes of this tract (Figure 2).

_____

Figure 2 about here

_____

The following steps were used: The ICBM fornix ROI was registered to MNI T1 template space using FSL's linear registration tool (FLIRT). Each participant's T1 image was then registered to the MNI T1 template using FSL's non-linear registration tool (FNIRT). Using the inverse transformation matrix and inverse non-linear warping parameters, the template space left fornix mask was then registered back to each participant's native space, effectively aligning it with their native space T1 image. T1 images were then segmented into GM, WM and CSF compartments and participants' fornix ROI masks were applied to their segmented WM images. Left fornix volumes were calculated based on the total

number of voxels labeled as WM within each participant's native space left fornix ROI (1 voxel = $1mm^3$). Each participant's resulting fornix volume was then 'normalized' (divided by their ICV).

2.7. Statistical analysis

All ROI analyses were conducted in SPSS 21.0 (Chicago, IL). Partial Pearson correlations were run controlling for age, sex and years of education. Initial ROI analyses focused on potential relationships between FA (the most general DTI measure of WM integrity) in each ROI and CSF protein levels. To limit the number of comparisons, relationships between more specific component diffusivity measures (DR/DA/MD) and CSF analytes were only explored in the presence of significant FA-CSF relationships. Partial correlations were also performed between CSF protein levels and the structural volumetric ROI data. Because we had no *a priori* hypotheses about laterality for the volumetric analyses, these correlations were run on the averaged normalized volumes in each ROI (e.g., the average of left and right hippocampus) and CSF protein level (e.g., $A\beta_{42}$), controlling for age, sex and education. There were two ROIs for each of the WM integrity (left fornix and left cingulum) and the GM volumetric (averaged left-right hippocampus and averaged left-right ERC) analyses. Thus, a family-wise significance level of $P = 0.025$ (i.e. $0.05/2$) was adopted for each of the WM integrity and volumetric ROI analyses.

We further sought to determine the potential influence of GM and WM volume in relevant MTL structures on significant WM-CSF relationships. This was explored by controlling for normalized volume of relevant GM or WM structures in the case of significant DTI-CSF partial correlations (i.e., adding left hippocampus volume or left fornix volume to the significant left fornix WM integrity – CSF models). Finally, the functional

relevance of significant DTI–CSF associations was explored through partial correlations between FA in that ROI and two UDS cognitive test scores of high relevance to preclinical AD states (Logical Memory Delayed and Digit Symbol) (Blacker, et al., 2007, Dickerson, et al., 2007), as well as a control measure of psychomotor speed (Trails A). To limit the number of comparisons, relationships between other more specific component diffusivity measures (DR/DA/MD) and these cognitive tests were only explored in the presence of significant FA-cognitive score relationships.

To supplement significant correlational findings in the fornix ROI, follow-up group comparisons were run by classifying individuals into high risk and low risk groups for preclinical AD based CSF $A\beta_{42}$ values. The cut-point values used were those established by Sjogren M et al. (2001) for INNOTEST® ELISA kits with 21F12 antibody for capture and 3D6 (biotinylated) antibody for detection of $A\beta_{42}$. These authors established a CSF $A\beta_{42}$ value of < 500 ng/L as cut-point for CN adults. Using this cut-point, 9 out of 20 of our participants were classified as high risk for preclinical AD.

Following ROI analyses, a voxelwise analysis was run in FSL to identify additional potential relationships between CSF measures and WM integrity in regions other than our ROIs. To limit the number of comparisons, we focused on the measures showing the most robust effects in our ROI analyses: FA and the $A\beta_{42}$/p-Tau_{181} ratio. The voxelwise analysis used linear regression with FA as the dependent variable, $A\beta_{42}$/p-Tau_{181} ratio as the independent variable of interest, and age, sex and education as covariates of no interest. A voxelwise permutation nonparametric test (using 5000 permutations) was employed using FSL's threshold-free cluster enhancement (TFCE). We expected DTI-CSF correlations to be subtle in our sample of CN participants. Thus, results were thresholded at $P < 0.001$

(uncorrected) and cluster size of ≥ 10 voxels. The statistical map was dilated for visualization purposes using the FSL function tbss_fill.

3. Results

3.1 *Demographic and Neuropsychological Characteristics*

The demographic and neuropsychological characteristics of the sample were consistent with a well-educated group of CN older adults (Table 1). The mean Mini-Mental State Examination score was 29.5 and none of the participants had an MMSE score below 27.

_____

Table 1 about here

_____

3.2. *ROI results*

There was a positive partial correlation between FA in the left fornix and both CSF $A\beta_{42}$ (r = 0.63, p = 0.003) (Figure 3, panel A) and $A\beta_{42}$/p-Tau_{181} ratio (r = 0.55, p = 0.01) (Figure 3, panel B). In contrast, there was no correlation between left hippocampal volume and either CSF $A\beta_{42}$ (r = 0.12, p = 0.64) (Figure 3, panel C) or $A\beta_{42}$/p-Tau_{181} (r = -0.10, p = 0.70) (Figure 3, panel D). In addition, the relationships between FA in the left fornix and CSF measures of $A\beta_{42}$ remained significant when normalized left hippocampal volume was controlled ($A\beta_{42}$, r = 0.62, p = 0.011; $A\beta_{42}$/p-Tau_{181} ratio, r = 0.59, p = 0.017) and when normalized left fornix volume was controlled ($A\beta_{42}$, r = 0.63, p = 0.010; $A\beta_{42}$/p-Tau_{181} ratio, r = 0.58, p = 0.018).

_____

Figure 3 about here

These effects in the fornix ROI were further confirmed with ANCOVAs in which participants were classified as high risk or low risk for preclinical AD based on based CSF $A\beta_{42}$ values (as described in the methods section). The high risk group had lower FA in the left fornix ROI, $F(1, 15) = 10.17$, $p = 0.006$. This group difference in the left fornix remained significant when normalized left hippocampal volume was controlled, $F(1, 14) = 9.85$, $p = 0.007$ and when normalized left fornix volume was controlled, $F(1, 14) = 9.61$, $p = 0.008$.

There were trends for negative partial correlations between DR in the left fornix and both $A\beta_{42}$/p-Tau_{181} ratio ($r = -0.50$, $p = 0.046$) and $A\beta_{42}$ ($r = -0.44$, $p = 0.09$), but neither met FWE corrected significance. Neither DA nor MD in the left fornix correlated with any CSF biomarkers (p-values ≥ 0.25). There was no correlation between FA in the left fornix and CSF p-Tau_{181} ($r = -0.01$, $p = 0.98$). There were no correlations between FA in the left cingulum and any of the CSF analytes ($P \geq 0.17$). There were no correlations between normalized hippocampal or ERC volumes and any CSF biomarkers (p-values ≥ 0.40).

There was a positive partial correlation between FA in the left fornix and scores on the Digit Symbol ($r = 0.50$, $p = 0.025$) and a negative partial correlation between DR in the left fornix and scores on the Digit Symbol ($r = -0.63$, $p = 0.004$). Scatter plots of the residual associations between WM integrity in the left fornix and Digit Symbol performance after controlling for age, sex, and education are displayed in Figure 4. In contrast, Digit Symbol scores were not correlated with normalized left hippocampal volume ($r = -0.24$, $p = 0.31$). In addition, the relationships between FA and DR in the left fornix and scores on the Digit Symbol remained significant when normalized left hippocampal volume was controlled (FA, $r = 0.52$, $p = 0.02$; DR, $r = -0.59$, $p = 0.011$). There were no statistically

significant correlations for either FA or DR in the Fornix and Logical Memory Delayed or Trails A (*p*-values ≥ 0.15).

Figure 4 about here

3.3. *Voxelwise results*

The $A\beta_{42}$/p-Tau_{181} ratio was positively correlated with FA in bilateral portions of the fornix, superior longitudinal fasciculus (SLF), and inferior fronto-occipital fasciculus (IFOF), as well as in the corpus callosum, and the left inferior longitudinal fasciculus (ILF) (Figure 5). Coordinates for the locations of peak significance in these regions are given in Table 2. When the results from the same analysis were corrected for multiple comparisons (using the FWE-correction method at $P < 0.05$), two clusters in the right SLF remained significant (MNI peak coordinates: 37 -13 31 and 30 -12 45). There were no negative correlations between the $A\beta_{42}$/p-Tau_{181} ratio and FA.

Figure 5 and Table 2 about here

4. Discussion

We observed a positive correlation between CSF measures of Aβ ($A\beta_{42}$ and $A\beta_{42}$/p-Tau_{181}) and cerebral WM integrity in cognitively normal (CN) older adults. In the crus region of the left fornix, the relationship between CSF measures of Aβ and WM microstructural integrity persisted after controlling for both hippocampal volume and fornix volume. Our results

suggest that *in vivo* WM integrity measures hold promise as non-invasive markers of preclinical AD.

Our ROI results link WM integrity in the fornix with CSF measures of amyloid beta ($A\beta_{42}$ and $A\beta_{42}$/p-Tau_{181}) in CN older adults. In contrast, no relationship was observed between WM integrity in our fornix ROI and CSF levels of p-Tau_{181}. The predominant AD biomarker time course model holds that the accumulation of Aβ, as measured by CSF $A\beta_{42}$ or amyloid imaging, is a key precipitating event in the pathophysiological cascade leading to tau-mediated neuronal injury, cerebral atrophy and memory impairment (Jack, et al., 2010). A more recent review maintains the view of Aβ as a likely initiator in sporadic AD, but suggests that tau pathologies may arise independently in some cases and remain beneath current *in vivo* CSF detection thresholds for longer than Aβ (Jack et al., 2013).

In either case, the present link between WM integrity in the fornix and measures of CSF $A\beta_{42}$ in CN older adults suggests that microstructural fornix damage may be an early event in the course of AD. As a further test of this possibility, we compared FA values in our fornix ROI between individuals classified according to CSF $A\beta_{42}$ values reflecting the likelihood of having preclinical AD according to values established by Sjogren et al. (2001). These authors used a rank-based method to estimate the lower reference limit for CSF $A\beta_{42}$ in CN adults. Using the cut-point of 500 ng/L established by these authors to classify our participants, we found lower WM integrity in our fornix ROI in the group likely to have preclinical AD compared to the group unlikely to have preclinical AD.

Our results are the first to our knowledge to link measures of WM integrity and CSF collected at the same time in CN older adults. A recent study reported correlations between measures of total tau (T-Tau and T-Tau/$A\beta_{42}$) and DTI measures collected approximately

3.5 years later in CN older adults (Bendlin, et al., 2012). These authors found that measures of CSF tau were correlated with DTI measures across much of the brain's WM, while CSF $A\beta_{42}$ was correlated with FA in the medial frontal gyrus. Although the relationship we observed between measures of CSF $A\beta_{42}$ and WM integrity in the fornix of CN older adults is novel, it appears to be broadly consistent with recent results reporting a similar relationship using PiB amyloid imaging (Chao, et al., 2013). These authors reported that PiB positive individuals (most of whom had aMCI) had lower WM integrity in the fornix (and splenium) than PiB-negative individuals (most of whom were CN).

The fornix is a key efferent tract of the hippocampus, connecting it with subcortical structures in the diencephalon and basal frontal lobes. However, the CSF-WM integrity relationship we observed in the fornix does not appear to be a secondary consequence of AD-related hippocampal atrophy (i.e., Wallerian degeneration) because the inclusion of hippocampal volume as an additional nuisance covariate did not affect the significance of our correlations between measures of CSF $A\beta_{42}$ and WM integrity in the fornix. These results are consistent with recent findings suggesting that alterations in the fornix are apparent in early stages of AD and may be independent from GM alterations (Gold et al., 2010; Oishi et al., 2012; Fletcher et al., 2013; Sachdev et al., 2013; Zhuang et al., 2013). The finding that the relationship between CSF $A\beta_{42}$ and WM integrity in the crus region persisted after controlling for fornix volume suggests that DTI may provide information about preclinical stages of AD that is not captured by traditional neuroimaging measures of WM macrostructure.

Results from our exploratory voxelwise analyses indicated a positive correlation between $A\beta_{42}$/p-Tau_{181} and FA in bilateral portions of the fornix, the SLF, and the IFOF, as

well as in the corpus callosum, and the left ILF. These voxelwise correlations are considered preliminary because only the right SLF survived correction for multiple comparisons. It should also be noted that the voxelwise effects were in a more rostral portion of the fornix (the body) than that observed in our ROI analyses (the crus). Multiple portions of the fornix are likely to be affected in preclinical AD. The crus is a thinner portion of the fornix than the body and thus less likely to meet significance and cluster thresholds required for voxelwise analyses. Nevertheless, the present link between CSF markers of AD and WM integrity in the fornix ROI is notable in that it represents a replication of a similar effect in this region observed in a different group of CN older adults in our previous work. Replication is acknowledged as a key step in the development of neuroimaging biomarkers of preclinical AD (Sperling, et al., 2011; Dickerson et al., 2012).

We note several caveats of the present study. First, our relatively small sample size may have limited the power to identify the full complement of WM patterns associated with CSF measures of Aβ in CN individuals. Another caveat is that DTI-based WM integrity effects in the fornix reported here and elsewhere may suffer from free water contamination due to the proximity of this tract to ventricular spaces. Future research should be directed toward answering this issue. It should also be acknowledged that our cross-sectional design yielded correlational results that cannot distinguish between the possibilities that Aβ accumulation could lead to myelin breakdown (Xu, et al., 2001) or that myelin breakdown could lead to AD pathogenesis (Bartzokis, 2011). Future longitudinal research may be able to distinguish between these possibilities by obtaining repeat-measure scans and lumbar punctures and determining which measure's decline rate better predicts the other.

Additional caveats should also be noted. First, our analyses focused initially on FA, with analyses of component diffusivities only being conducted in the presence of significant FA-CSF relationships. The FA-first analysis stream was selected because FA is considered a general measure of WM integrity and served to limit the number of comparisons conducted. However, component diffusivity effects have sometimes been reported as more prominent than FA effects (Acosta-Cabronero et al., 2010; Fletcher et al., 2013) and our approach may have missed some component diffusivity effects occurring in the absence of FA effects. Another caveat is that we did not compute total tau and were thus unable to assess possible relationships between levels of CSF protein and WM integrity in CN older adults. Finally, future longitudinal studies will be required to assess relationships between rates of change in WM integrity, CSF levels and cognition.

In summary, our results suggest a link between measures of cerebral WM integrity and CSF markers of AD pathology in CN older adults. In particular, our findings suggest that presumed early degenerative changes affecting the fornix in CN older adults may be independent of those affecting the hippocampus and cannot be accounted for by fornix volume. Future DTI studies with larger sample sizes hold promise for identifying potential WM integrity biomarkers of AD in its earliest stages.

Acknowledgements

This study was supported by the National Institute on Aging of the National Institutes of Health under award numbers (P30 AG028383, P01 AG030128, R01 AG033036). The content is solely the responsibility of the authors and does not necessarily represent the official views of these granting agencies. We thank Beverly Meacham for her assistance in scanning participants. Most of all, we wish to thank the dedicated volunteers at the Sanders-Brown Center on Aging for their participation in this research.

Tables

Table 1. Demographic data, psychometric test scores and CSF $A\beta_{42}$ values of the participants

N = 20	Mean (SD)
Age, years	76.2 (5.8)
Sex, male/female number	8/12
Education, years	16.7 (2.5)
MMSE	29.5 (0.8)
Fluency Animals	21.0 (6.2)
Trails A	32.7 (12.3)
Trails B	81.6 (48.1)
LM Imm	16.8 (3.0)
LM Del	16.1 (3.1)
Digit Symbol	48.8 (11.0)
APOE4, yes/no	6/14
CSF $A\beta_{42}$ values (pg/mL)	502 (219)

Notes: MMSE, Mini Mental State Examination; LM Imm, immediate recall of Logical Memory; LM Del, delayed recall of Logical Memory.

Table 2. White matter regions showing a positive correlation between FA and the CSF $A\beta_{1\text{-}42}$/p-tau_{181} ratio.

White Matter Tract	MNI coordinate			Peak *T* value
	x	y	z	
Left Fornix	-6	-13	13	4.51
Left genu of the corpus callosum	-9	21	-7	4.24
Left Inferior Longitudinal Fasciculus	-46	-21	-18	4.82
Left Inferior Fronto-Occipital Fasciculus	-23	-83	6	4.06
Left Superior Longitudinal Fasciculus	-16	21	44	3.86
Right Fornix	9	-15	13	4.42
Right Inferior Fronto-Occipital Fasciculus	21	-80	21	4.53
Right Superior Longitudinal Fasciculus	38	-15	31	4.97
Right Superior Longitudinal Fasciculus	18	-40	57	4.31
Right Superior Longitudinal Fasciculus	18	14	55	5.22
Right Superior Longitudinal Fasciculus	30	-10	54	5.83

Notes: MNI, Montreal Neurological Institute; Tract identification was aided by the JHU ICBM-DT-81 White Matter Labels and JHU White-Matter Tractography Atlases.

Figure Legends

Figure 1. A representation of the *a priori* left fornix and left cingulum regions of interest (ROIs). The image is a coronal slice showing regions of lower WM integrity (in red) associated with AD-risk in one of our previous studies. The number below the slice represents its y coordinate in MNI space. The labeled regions represent the approximate center of each ROI's y coordinate in MNI space (see methods for details). Notes: L, left; R, right. CING, cingulum.

Figure 2. Illustration of steps used to compute fornix volume on a representative participant. The left column shows a lateral portion of the left fornix and the right column shows a medial portion of the left fornix (the body). A participant's ICBM DTI left fornix mask was registered to their native space T1 image (A). The participant's T1 image was segmented to obtain their WM image (B). The participant's fornix mask was registered to their segmented WM image (C), restricting the volumetric measurement to WM.

Figure 3. Fornix and hippocampal ROI measures plotted against CSF measures of Aβ. Scatter plots show residual associations after controlling for age, sex and education. Positive correlations were observed between FA in the left fornix and both CSF $A\beta_{42}$ (panel A) and $A\beta_{42}$/p-Tau_{181} ratio (panel B). In contrast, there was no correlation between left hippocampal volume and either CSF $A\beta_{42}$ (panel C) or $A\beta_{42}$/p-Tau_{181} ratio (panel D). Units on the X and Y axes represent residual values that have been standardized within our sample (set to a mean of zero and a standard deviation of one). Note: *$p < 0.05$; **$p < 0.01$.

Figure 4. Measures of WM integrity in the fornix ROI plotted against scores on the Digit Symbol (DS) test. Scatter plots show residual associations after controlling for age, sex and education. There was a positive correlation between FA in the fornix and DS score (panel A) and a negative correlation between DR in the fornix and DS score (panel B). Units on the X and Y axes represent residual values that have been standardized within our sample (set to a mean of zero and a standard deviation of one). Note: *$p < 0.05$; **$p < 0.01$.

Figure 5. Results of voxelwise regression analysis. Positive correlations (in red) were observed between the $A\beta_{42}$/p-Tau_{181} ratio and FA after controlling for age, sex and education. The common tract skeleton is in green. The numbers below each slice represent y coordinates in MNI space and the coordinates for the locations of peak significance in these regions are given in Table 2. Notes: L, left; R, right; SLF, superior longitudinal fasciculus; IFOF, inferior fronto-occipital fasciculus; ILF, inferior longitudinal fasciculus.

References

Acosta-Cabronero, J. Williams, G.B., Pengas, G., Nestor, P.J., 2010. Absolute diffusivities define the landscape of white matter degeneration in Alzheimer's disease. Brain 133,529-539.

Apostolova, L.G., Mosconi, L., Thompson, P.M., Green, A.E., Hwang, K.S., Ramirez, A., Mistur, R., Tsui, W.H., de Leon, M.J., 2010. Subregional hippocampal atrophy predicts Alzheimer's dementia in the cognitively normal. Neurobiol Aging 31, 1077-88.

Bartzokis, G., 2011. Alzheimer's disease as homeostatic responses to age-related myelin breakdown. Neurobiol Aging 32, 1341-71.

Basser, P.J., Pajevic, S., Pierpaoli, C., Duda, J., Aldroubi, A., 2000. In vivo fiber tractography using DT-MRI data. Magn Reson Med 44, 625-32.

Beaulieu, C., 2002. The basis of anisotropic water diffusion in the nervous system - a technical review. NMR Biomed 15, 435-55.

Bendlin, B.B., Carlsson, C.M., Johnson, S.C., Zetterberg, H., Blennow, K., Willette, A.A., Okonkwo, O.C., Sodhi, A., Ries, M.L., Birdsill, A.C., Alexander, A.L., Rowley, H.A., Puglielli, L., Asthana, S., Sager, M.A., 2012. CSF T-Tau/Abeta42 predicts white matter microstructure in healthy adults at risk for Alzheimer's disease. PLoS One 7, e37720.

Bendlin, B.B., Ries, M.L., Canu, E., Sodhi, A., Lazar, M., Alexander, A.L., Carlsson, C.M., Sager, M.A., Asthana, S., Johnson, S.C., 2010. White matter is altered with parental family history of Alzheimer's disease. Alzheimers Dement 6, 394-403.

Bennett, D.A., Schneider, J.A., Arvanitakis, Z., Kelly, J.F., Aggarwal, N.T., Shah, R.C., Wilson, R.S., 2006. Neuropathology of older persons without cognitive impairment from two community-based studies. Neurology 66, 1837-44.

Bennett, I.J., Madden, D.J., Vaidya, C.J., Howard, D.V., Howard, J.H., Jr., 2010 Age-related differences in multiple measures of white matter integrity: A diffusion tensor imaging study of healthy aging. Hum Brain Mapp 31, 378-390.

Blacker, D., Lee, H., Muzikansky, A., Martin, E.C., Tanzi, R., McArdle, J.J., Moss, M., Albert, M., 2007. Neuropsychological measures in normal individuals that predict subsequent cognitive decline. Arch Neurol 64, 862-71.

Bronge, L., Bogdanovic, N., Wahlund, L.O., 2002. Postmortem MRI and histopathology of white matter changes in Alzheimer brains. A quantitative, comparative study. Dement Geriatr Cogn Disord 13, 205-12.

Brun, A., Englund, E., 1986. A white matter disorder in dementia of the Alzheimer type: a pathoanatomical study. Ann Neurol 19, 253-62.

Chao, L.L., Decarli, C., Kriger, S., Truran, D., Zhang, Y., Laxamana, J., Villeneuve, S., Jagust, W.J., Sanossian, N., Mack, W.J., Chui, H.C., Weiner, M.W., 2013. Associations between White Matter Hyperintensities and beta Amyloid on Integrity of Projection, Association, and Limbic Fiber Tracts Measured with Diffusion Tensor MRI. PloS one 8, e65175.

Convit, A., De Leon, M.J., Tarshish, C., De Santi, S., Tsui, W., Rusinek, H., George, A., 1997. Specific hippocampal volume reductions in individuals at risk for Alzheimer's disease. Neurobiol Aging 18, 131-8.

de Leon, M.J., DeSanti, S., Zinkowski, R., Mehta, P.D., Pratico, D., Segal, S., Rusinek, H., Li, J., Tsui, W., Saint Louis, L.A., Clark, C.M., Tarshish, C., Li, Y., Lair, L., Javier, E., Rich, K., Lesbre, P., Mosconi, L., Reisberg, B., Sadowski, M., DeBernadis, J.F., Kerkman, D.J., Hampel, H., Wahlund, L.O., Davies, P., 2006. Longitudinal CSF and MRI biomarkers improve the diagnosis of mild cognitive impairment. Neurobiol Aging 27, 394-401.

Desikan, R.S., Segonne, F., Fischl, B., Quinn, B.T., Dickerson, B.C., Blacker, D., Buckner, R.L., Dale, A.M., Maguire, R.P., Hyman, B.T., Albert, M.S., Killiany, R.J., 2006. An automated labeling system for subdividing the human cerebral cortex on MRI scans into gyral based regions of interest. Neuroimage 31, 968-80.

Dickerson, B.C., Sperling, R.A., Hyman, B.T., Albert, M.S., Blacker, D., 2007. Clinical prediction of Alzheimer disease dementia across the spectrum of mild cognitive impairment. Arch Gen Psychiatry 64, 1443-50.

Dickerson, B.C., Wolk, D.A., 2012. MRI cortical thickness biomarker predicts AD-like CSF and cognitive decline in normal adults. Neurology 78, 84-90.

Englund, E., 1998. Neuropathology of white matter changes in Alzheimer's disease and vascular dementia. Dement Geriatr Cogn Disord 9, 6-12.

Fischl, B., Salat, D.H., Busa, E., Albert, M., Dieterich, M., Haselgrove, C., van der Kouwe, A., Killiany, R., Kennedy, D., Klaveness, S., Montillo, A., Makris, N., Rosen, B., Dale, A.M., 2002. Whole brain segmentation: automated labeling of neuroanatomical structures in the human brain. Neuron 33, 341-55.

Fischl, B., van der Kouwe, A., Destrieux, C., Halgren, E., Segonne, F., Salat, D.H., Busa, E., Seidman, L.J., Goldstein, J., Kennedy, D., Caviness, V., Makris, N., Rosen, B., Dale, A.M., 2004. Automatically parcellating the human cerebral cortex. Cerebral Cortex 14, 11-22.

Fjell, A.M., Walhovd, K.B., Fennema-Notestine, C., McEvoy, L.K., Hagler, D.J., Holland, D., Blennow, K., Brewer, J.B., Dale, A.M., Initi, A.s.D.N., 2010. Brain Atrophy in Healthy Aging Is Related to CSF Levels of A beta 1-42. Cerebral Cortex 20, 2069-79.

Fletcher, E., Raman, M., Huebner, P., Liu A., Mungas, D., Carmichael, O., DeCarli, C., 2013. Loss of fornix white matter volume as a predictor of cognitive impairment in cognitively normal elderly individuals. JAMA neurology 70, 1389-1395.

Gold, B.T., Johnson, N.F., Powell, D.K., Smith, C.D., 2012. White matter integrity and vulnerability to Alzheimer's disease: preliminary findings and future directions. Biochim Biophys Acta 1822, 416-22.

Gold, B.T., Powell, D.K., Andersen, A.H., Smith, C.D., 2010. Alterations in multiple measures of white matter integrity in normal women at high risk for Alzheimer's disease. Neuroimage 52, 1487-94.

Heise, V., Filippini, N., Ebmeier, K.P., Mackay, C.E., 2011. The APOE varepsilon4 allele modulates brain white matter integrity in healthy adults. Mol Psychiatry 16, 908-16.

Ihara, M., Polvikoski, T.M., Hall, R., Slade, J.Y., Perry, R.H., Oakley, A.E., Englund, E., O'Brien, J.T., Ince, P.G., Kalaria, R.N., 2010. Quantification of myelin loss in frontal lobe white matter in vascular dementia, Alzheimer's disease, and dementia with Lewy bodies. Acta Neuropathol 119, 579-89.

Jack, C.R., Jr., Knopman, D.S., Jagust, W.J., Petersen, R.C., Weiner, M.W., Aisen, P.S., Shaw, L.M., Vemuri, P., Wiste, H.J., Weigand, S.D., Lesnick, T.G., Pankratz, V.S., Donohue, M.C., Trojanowski, J.Q., 2013. Tracking pathophysiological processes in Alzheimer's disease: an updated hypothetical model of dynamic biomarkers. Lancet Neurol 12, 207-216.

Jack, C.R., Jr., Knopman, D.S., Jagust, W.J., Shaw, L.M., Aisen, P.S., Weiner, M.W., Petersen, R.C., Trojanowski, J.Q., 2010. Hypothetical model of dynamic biomarkers of the Alzheimer's pathological cascade. Lancet Neurol 9, 119-28.

Jack, C.R., Jr., Petersen, R.C., Xu, Y.C., Waring, S.C., O'Brien, P.C., Tangalos, E.G., Smith, G.E., Ivnik, R.J., Kokmen, E., 1997. Medial temporal atrophy on MRI in normal aging and very mild Alzheimer's disease. Neurology 49, 786-94.

Johnson, N.F., Kim, C., Clasey, J.L., Bailey, A., Gold, B.T., 2012. Cardiorespiratory fitness is positively correlated with cerebral white matter integrity in healthy seniors. Neuroimage 59, 1514-23.

Joy, S., Kaplan, E., Fein, D., 2003. Digit Symbol-Incidental Learning in the WAIS-III: construct validity and clinical significance. Clin Neuropsychol 17, 182-94.

Le Bihan, D., 2003. Looking into the functional architecture of the brain with diffusion MRI. Nat Rev Neurosci 4, 469-80.

Martin, S.B., Smith, C.D., Collins, H.R., Schmitt, F.A., Gold, B.T., 2010. Evidence that volume of anterior medial temporal lobe is reduced in seniors destined for mild cognitive impairment. Neurobiol Aging 31, 1099-106.

McKhann, G.M., Knopman, D.S., Chertkow, H., Hyman, B.T., Jack, C.R., Jr., Kawas, C.H., Klunk, W.E., Koroshetz, W.J., Manly, J.J., Mayeux, R., Mohs, R.C., Morris, J.C., Rossor, M.N., Scheltens, P., Carrillo, M.C., Thies, B., Weintraub, S., Phelps, C.H., 2011. The diagnosis of dementia due to Alzheimer's disease: recommendations from the National Institute on Aging-Alzheimer's Association workgroups on diagnostic guidelines for Alzheimer's disease. Alzheimers Dement 7, 263-9.

Morris, J.C., Storandt, M., McKeel, D.W., Jr., Rubin, E.H., Price, J.L., Grant, E.A., Berg, L., 1996. Cerebral amyloid deposition and diffuse plaques in "normal" aging: Evidence for presymptomatic and very mild Alzheimer's disease. Neurology 46, 707-19.

Morris, J.C., Weintraub, S., Chui, H.C., Cummings, J., Decarli, C., Ferris, S., Foster, N.L., Galasko, D., Graff-Radford, N., Peskind, E.R., Beekly, D., Ramos, E.M., Kukull, W.A., 2006. The Uniform Data Set (UDS): clinical and cognitive variables and descriptive data from Alzheimer Disease Centers. Alzheimer Dis Assoc Disord 20, 210-216.

Moseley, M., 2002. Diffusion tensor imaging and aging - a review. NMR Biomed 15, 553-60.

Oishi, K., Mielke, M.M., Albert, M., Lyketsos, C.G., Mori S., 2012. The fornix sign: a potential sign for Alzheimer's disease based on diffusion tensor imaging. J Neuroimaging 22, 365-374.

Persson, J., Lind, J., Larsson, A., Ingvar, M., Cruts, M., Van Broeckhoven, C., Adolfsson, R., Nilsson, L.G., Nyberg, L., 2006. Altered brain white matter integrity in healthy carriers of the APOE epsilon4 allele: a risk for AD? Neurology 66, 1029-33.

Ringman, J.M., O'Neill, J., Geschwind, D., Medina, L., Apostolova, L.G., Rodriguez, Y., Schaffer, B., Varpetian, A., Tseng, B., Ortiz, F., Fitten, J., Cummings, J.L., Bartzokis, G., 2007. Diffusion tensor imaging in preclinical and presymptomatic carriers of familial Alzheimer's disease mutations. Brain 130, 1767-76.

Roher, A.E., Weiss, N., Kokjohn, T.A., Kuo, Y.M., Kalback, W., Anthony, J., Watson, D., Luehrs, D.C., Sue, L., Walker, D., Emmerling, M., Goux, W., Beach, T., 2002. Increased A beta peptides and reduced cholesterol and myelin proteins characterize white matter degeneration in Alzheimer's disease. Biochemistry 41, 11080-90.

Sachdev, P.S., Zhuang, L., Braidy, N., Wen, W., 2013. Is Alzheimer's a disease of the white matter? Current opinion in psychiatry 26, 244-251.

Schmitt, F.A., Nelson, P.T., Abner, E., Scheff, S., Jicha, G.A., Smith, C., Cooper, G., Mendiondo, M., Danner, D.D., Van Eldik, L.J., Caban-Holt, A., Lovell, M.A., Kryscio, R.J., 2012. University of Kentucky Sanders-Brown healthy brain aging volunteers: donor characteristics, procedures and neuropathology. Curr Alzheimer Res 9, 724-33.

Schott, J.M., Bartlett, J.W., Fox, N.C., Barnes, J., 2010. Increased Brain Atrophy Rates in Cognitively Normal Older Adults with Low Cerebrospinal Fluid A beta 1-42. Ann Neurol 68, 825-34.

Shahani, N., Brandt, R., 2002. Functions and malfunctions of the tau proteins. Cellular and molecular life sciences : CMLS 59, 1668-80.

Sjogren, M., Vanderstichele, H., Agren, H., Zachrisson, O., Edsbagge, M., Wikkelso, C., Skoog, I., Wallin, A., Wahlund, L.O., Marcusson, J., Nagga, K., Andreasen, N., Davidsson, P., Vanmechelen, E., Blennow, K. 2001. Tau and Abeta42 in cerebrospinal fluid from healthy adults 21-93 years of age: establishment of reference values. Clin Chem 47, 1776-1781.

Smith, C.D., Chebrolu, H., Andersen, A.H., Powell, D.A., Lovell, M.A., Xiong, S., Gold, B.T., 2010. White matter diffusion alterations in normal women at risk of Alzheimer's disease. Neurobiol Aging 31, 1122-31.

Smith, S.M., Jenkinson, M., Johansen-Berg, H., Rueckert, D., Nichols, T.E., Mackay, C.E., Watkins, K.E., Ciccarelli, O., Cader, M.Z., Matthews, P.M., Behrens, T.E., 2006. Tract-based spatial statistics: voxelwise analysis of multi-subject diffusion data. Neuroimage 31, 1487-505.

Sperling, R.A., Aisen, P.S., Beckett, L.A., Bennett, D.A., Craft, S., Fagan, A.M., Iwatsubo, T., Jack, C.R., Jr., Kaye, J., Montine, T.J., Park, D.C., Reiman, E.M., Rowe, C.C., Siemers, E., Stern, Y., Yaffe, K., Carrillo, M.C., Thies, B., Morrison-Bogorad, M., Wagster, M.V., Phelps, C.H., 2011. Toward defining the preclinical stages of Alzheimer's disease: recommendations from the National Institute on Aging-Alzheimer's Association workgroups on diagnostic guidelines for Alzheimer's disease. Alzheimers Dement 7, 280-92.

Stebbins, G.T., Murphy, C.M., 2009. Diffusion tensor imaging in Alzheimer's disease and mild cognitive impairment. Behav Neurol 21, 39-49.

Tosun, D., Schuff, N., Truran-Sacrey, D., Shaw, L.M., Trojanowski, J.Q., Aisen, P., Peterson, R., Weiner, M.W., 2010. Relations between brain tissue loss, CSF biomarkers, and the ApoE genetic profile: a longitudinal MRI study. Neurobiol Aging 31, 1340-54.

Wechsler, D.S., 1981. The Wechsler Adult Intelligence Scale--Revised. Psychological Corp, New York.

Weintraub, S., Salmon, D., Mercaldo, N., Ferris, S., Graff-Radford, N.R., Chui, H., Cummings, J., DeCarli, C., Foster, N.L., Galasko, D., Peskind, E., Dietrich, W., Beekly, D.L., Kukull, W.A., Morris, J.C.,

2009. The Alzheimer's Disease Centers' Uniform Data Set (UDS): the neuropsychologic test battery. Alzheimer Dis Assoc Disord 23, 91-101.

Xu, J., Chen, S., Ahmed, S.H., Chen, H., Ku, G., Goldberg, M.P., Hsu, C.Y., 2001. Amyloid-beta peptides are cytotoxic to oligodendrocytes. J Neurosci 21, RC118.

Zhuang, L., Sachdev, P.S., Trollor, J.N., Reppermund, S., Kochan, N.A., Brodaty, H., Wen, W., 2013 Microstructural white matter changes, not hippocampal atrophy, detect early amnestic mild cognitive impairment. PLoS One 8, e58887.

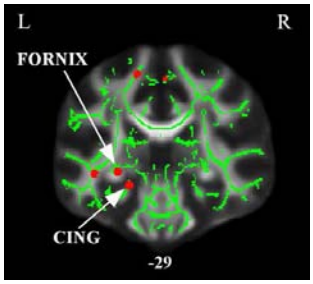

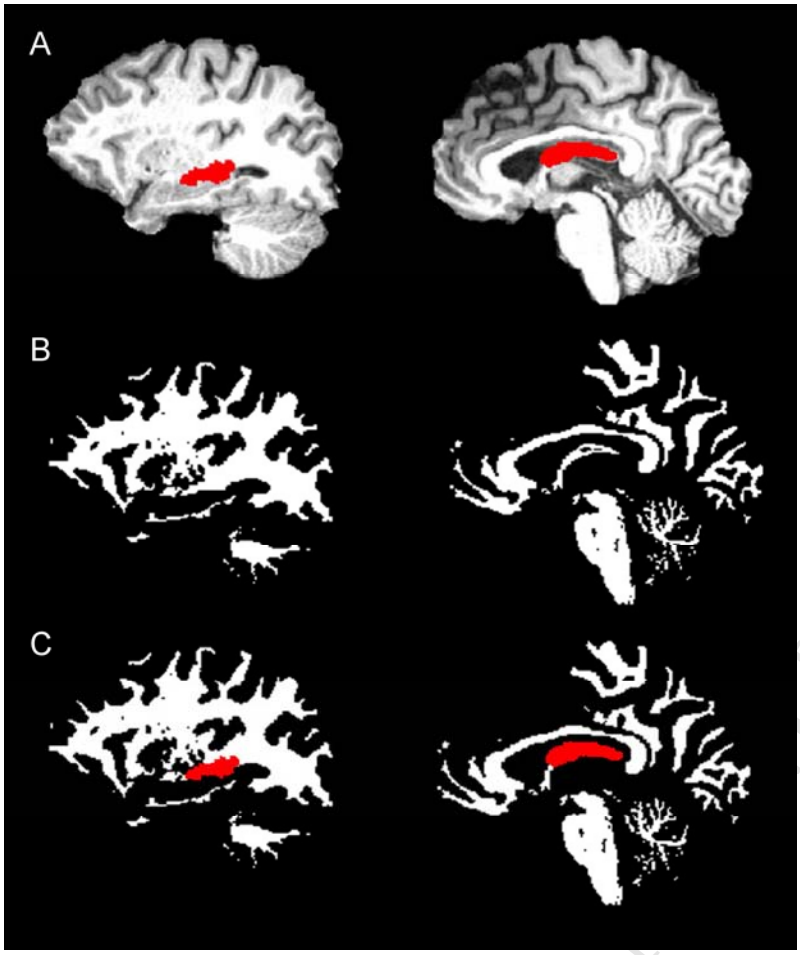

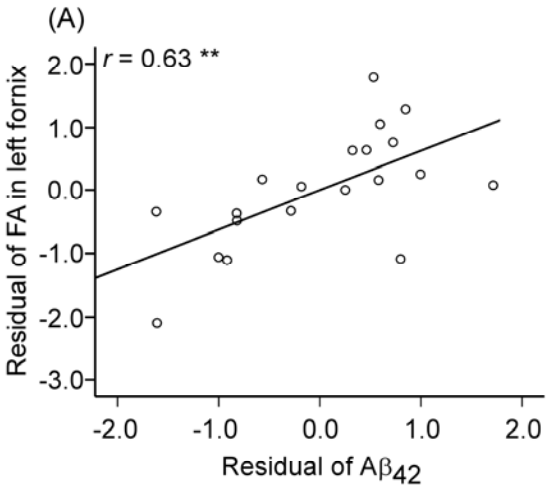
(A)
r = 0.63 **
Residual of FA in left fornix
Residual of Aβ42
2.0
1.0
0.0
-1.0
-2.0
-3.0
-2.0
-1.0
0.0
1.0
2.0

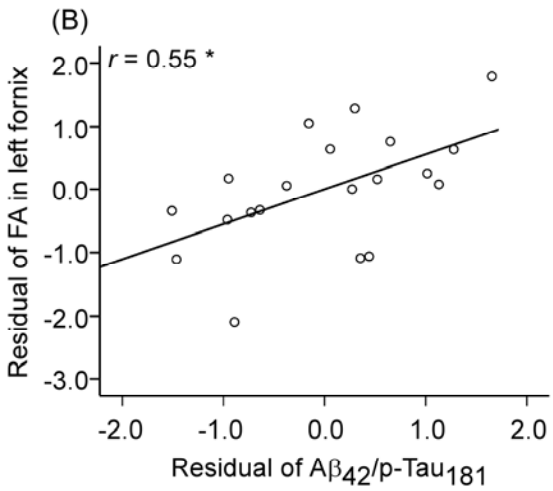
(B)
r = 0.55 *
Residual of FA in left fornix
Residual of Aβ42/p-Tau181
2.0
1.0
0.0
-1.0
-2.0
-3.0
-2.0
-1.0
0.0
1.0
2.0

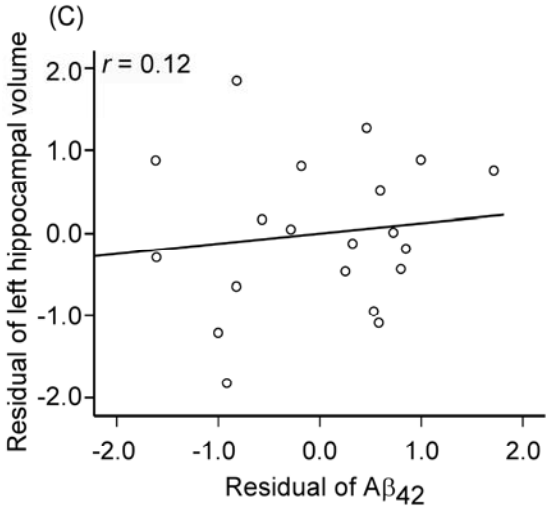
(C)
r = 0.12
Residual of left hippocampal volume
Residual of Aβ42
2.0
1.0
0.0
-1.0
-2.0
-2.0
-1.0
0.0
1.0
2.0

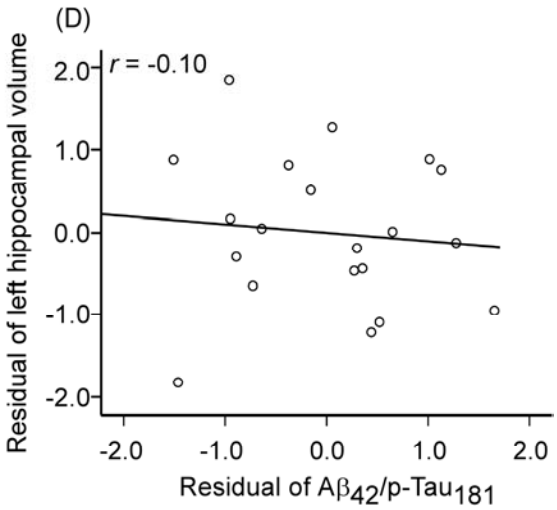
(D)
r = -0.10
Residual of left hippocampal volume
Residual of Aβ42/p-Tau181
2.0
1.0
0.0
-1.0
-2.0
-2.0
-1.0
0.0
1.0
2.0